JACS
JOURNAL OF THE AMERICAN CHEMICAL SOCIETY
pubs.acs.org/JACS
Communication

Pore Distortion in a Metal–Organic Framework for Regulated Separation of Propane and Propylene

Liang Yu,[○] Xue Han,[○] Hao Wang,* Saif Ullah, Qibin Xia, Weiyao Li, Jiangnan Li, Ivan da Silva, Pascal Manuel, Svemir Rudić, Yongqiang Cheng, Sihai Yang,* Timo Thonhauser, and Jing Li*

Cite This: https://doi.org/10.1021/jacs.1c10423
Read Online

ABSTRACT: The development of porous solids for adsorptive separation of propylene and propane remains an important and challenging line of research. State-of-the-art sorbent materials often suffer from the trade-off between adsorption capacity and selectivity. Here, we report the regulated separation of propylene and propane in a metal–organic framework *via* designed pore distortion. The distorted pore structure of HIAM-301 successfully excludes propane and thus achieved simultaneously high selectivity (>150) and large capacity (~3.2 mmol/g) of propylene at 298 K and 1 bar. Dynamic breakthrough measurements validated the excellent separation of propane and propylene. *In situ* neutron powder diffraction and inelastic neutron scattering revealed the binding domains of adsorbed propylene molecules in HIAM-301 as well as host–guest interaction dynamics. This study presents a new benchmark for the adsorptive separation of propylene and propane.

With a projected global production of 160 million metric tons by 2030, propylene plays a key role in the petrochemical industry for the manufacture of various consumer products.[1] Currently propylene is produced primarily *via* thermal or catalytic cracking of hydrocarbons where propane coexists as a byproduct, and many synthetic processes require the propylene stream with a purity of >99.5%.[2,3] Due to the small difference in the volatilities of propylene and propane, their separation by cryogenic distillation is identified as the most energy-intensive single distillation practiced commercially.[4] Thus, it is imperative to develop alternative separation methods with a lower energy input and suppressed carbon emission; adsorptive separation by porous solids at ambient conditions emerges as a promising solution.

Various adsorbents, such as zeolites, carbons, and other composite materials, have been explored for this separation.[2−6] Zeolite 4A and 5A adopt a pore aperture that is similar to the molecular dimensions of propane and propylene and can achieve the separation.[2] Zeolite 4A adsorbs propylene while excluding propane; however, the applicability is limited by its slow adsorption kinetics to propylene. In contrast, zeolite 5A is capable of accommodating both gases and discriminating them through thermodynamic separation but with very low selectivity of ~2.[7] Emerging metal–organic frameworks (MOFs) hold increasing promise for this separation owing to their highly tunable pore structures.[8,9] MOFs with target functional groups and/or pore dimensions can be designed through topology-directed pore size regulation. This is crucial for achieving the desired properties. A number of MOFs have been evaluated for propane/propylene separation, and some outperform traditional sorbents with improved separation efficiency.[8,10−12] These MOFs can be divided into two categories. The first category operates *via* specific adsorption sites to deliver the thermodynamic preference to propylene over propane.[13,14] For example, MOF-74/CPO-27 features abundant coordinatively unsaturated metal sites along its channel that can selectively bond to propylene over propane. The second family are those with optimal pore dimensions acting as splitters that exhibit kinetic separation or more ideally selective molecular exclusion, such as KAUST-7 and Co-gallate.[7,15−19] They can adsorb propylene but exclude propane due to restricted diffusion, behaving similarly to zeolite 4A.

To date, challenges remain in developing efficient sorbents with both a high adsorption capacity and selectivity. MOFs with unsaturated metal centers generally show limited selectivity upon the rapid saturation of these sites. On the contrary, the very few MOFs showing selective molecular exclusion feature a high selectivity but a naturally low adsorption capacity (typically <2 mmol/g) due to their restricted porosity. Here, we report a new MOF, $Y_6(OH)_8(eddi)_3(DMA)_2$ (denoted as HIAM-301, HIAM refers to Hoffmann Institute of Advanced Materials, H_4eddi = 5,5′-(ethene-1,2-diyl)diisophthalic acid, DMA = dimethylammonium), developed *via* reticular chemistry to achieve a precisely distorted pore structure. At 298 K and 1 bar, HIAM-301 fully excludes propane but adsorbs a large amount of propylene (3.2 mmol/g), notably higher than all previously reported sorbent materials that exhibit molecular exclusion of propane, including the best performing JNU-3a reported very recently.[19] Its excellent separation performance has been confirmed by multicycle breakthrough measurements. *In situ*

Received: October 1, 2021

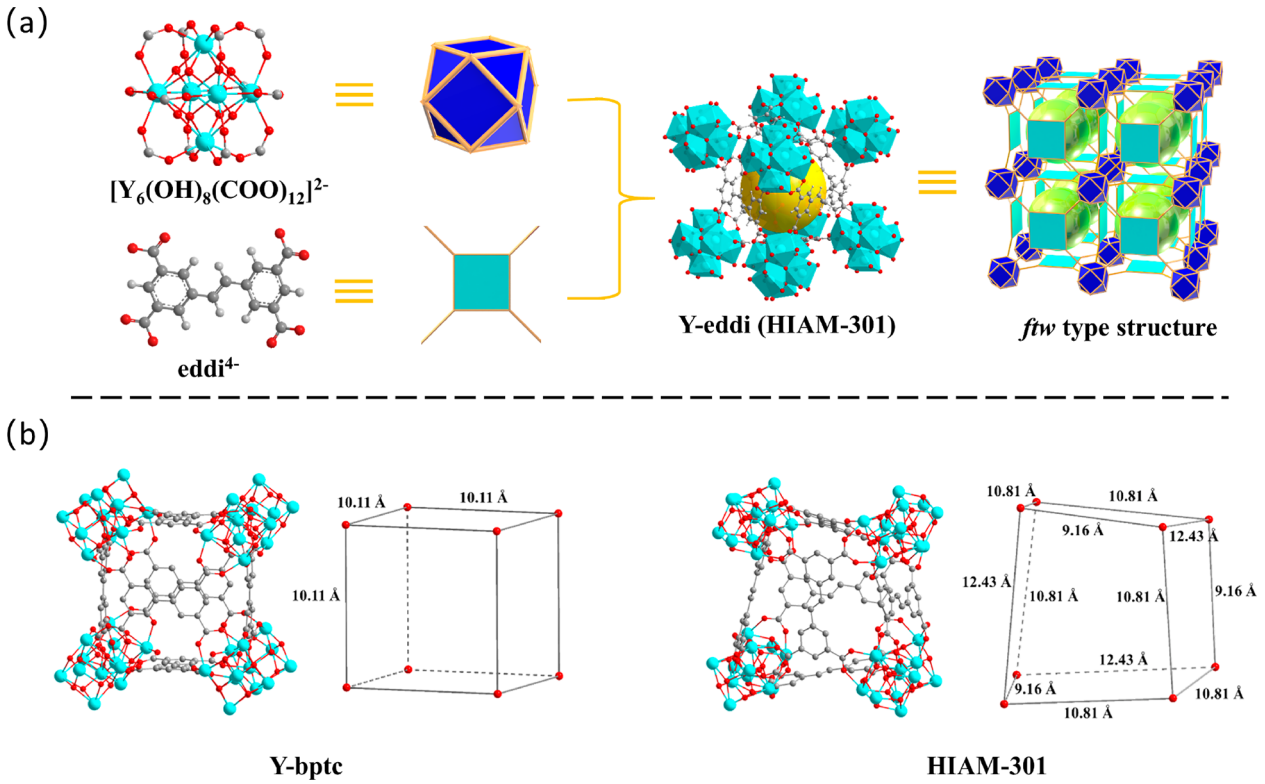

Figure 1. (a) Inorganic and organic building units, crystal structure, and topology of HIAM-301. (b) Pore distortion of HIAM-301 compared to the perfect cubic cage of Y-bptc and the shape of the cage depicted by connecting eight equivalent μ_3-O atoms from the vertexes.

neutron powder diffraction (NPD) and inelastic neutron scattering (INS) have enabled the direct observation of binding domains of adsorbed propylene molecules as well as host−guest binding dynamics, providing key insights into the separation mechanism.

The **ftw**-MOFs,[20−23] which are built from hexanuclear clusters M_6 (M = Zr^{4+}, Hf^{4+}, Ce^{4+}, Y^{3+}) and planar, tetratopic linkers, are advantageous for molecular separation as a result of their large cage-like cavities interconnected through narrow windows. The former guarantees a high adsorption capacity while the latter can discriminate molecules with different dimensions. However, the precise control of window size *via* a judicious choice of ligand alone is challenging since the synthesis of an organic linker with delicate dimensions can be impractical. Additional control on the pore size of **ftw**-MOFs can be achieved by modulating the framework charge *via* a replacement of Zr_6 clusters by Y_6 clusters. While the Zr-MOFs are charge-neutral, the isostructural Y-analogues feature an anionic framework with countercations residing in the cavities, acting as additional regulators of the pore aperture of **ftw**-MOFs.

Block-shaped crystals of HIAM-301 were synthesized solvothermally from $Y(NO_3)_3{\cdot}9H_2O$ and H_4eddi in DMF with the addition of 2-fluorobenzoic acid as a modulator. HIAM-301 crystallizes in the space group $R\bar{3}c$, with a formula of $Y_6(OH)_8(eddi)_3(DMA)_2$. The overall structure is built on 12-connected hexanuclear $Y_6(OH)_8(COO)_{12}$ and 4-connected eddi^{4-}. Each Y^{3+} is eight-coordinated to four μ_3-OH^- and four carboxylates from four different eddi^{4-} linkers. The hexanuclear clusters are interconnected through eddi^{4-} linkers, forming a 3D framework with distorted cubic cages interconnected through small windows (Figure 1 and Figure S1). As expected, HIAM-301 features a 4,12-c **ftw**-type topology; however, the cubic cage (as well as the pore aperture) in the structure is highly contracted and distorted compared to that in common **ftw**-type structures, such as Y-bptc (Figure 1b and Figures S2−S4). In an ideal 4,12-c **ftw** structure, the plane described by the four center of mass of the octahedrons and the one described by the ligand are coincident, which is not the case for HIAM-301 as a result of the mutual rotation of the octahedra and the geometry of the ligand (Figures S3 and S4). This can be attributed to the large aspect ratio (1.86) of the H_4eddi linker, which deviates notably from a square shape, resulting in the formation of a distorted pore structure with better control of guest accessibility. The excellent stability of HIAM-301 and its strong resistance toward thermal, moisture, and chemical environments have been confirmed by powder X-ray diffraction (PXRD) analysis (Figures S5−S7). In addition, adsorption measurements on the sample after water treatment for 1 week shows essentially no loss of adsopriton capacity (Figure S9).

The distorted cages in HIAM-301 feature 10 × 10 $Å^2$ cavities interconnected through small windows. The presence of DMA cations in the pore was confirmed by NMR studies (Figure S10) and their position was determined by NPD (see below). HIAM-301 exhibited little adsorption of N_2 at 77 K due to the active diffusion caused by the narrow pores.[24] Thus, the porosity of HIAM-301 was evaluated by CO_2 adsorption at 195 K (Figure S11). HIAM-301 exhibits a BET surface area of 579 m^2/g, a pore volume of 0.26 cm^3/g, and a pore size of 4.6 Å (Figure S12), slightly higher than that of Y-bptc,[21] which is constructed from a shorter ligand and gives no adsorption of propane or propylene.

Single-component adsorption isotherms of propane and propylene were collected for HIAM-301 (Figure 2a and Figure

https://doi.org/10.1021/jacs.1c10423
J. Am. Chem. Soc. XXXX, XXX, XXX−XXX

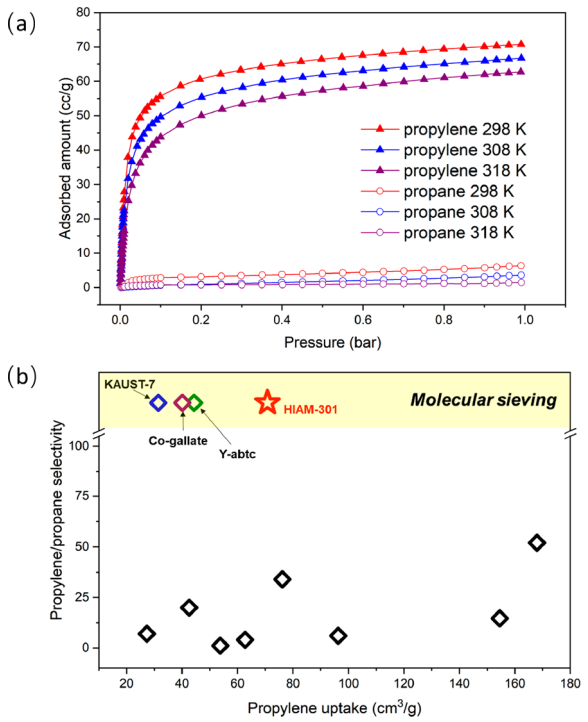

Figure 2. (a) Adsorption isotherms of propylene and propane on HIAM-301 at 298, 308, and 318 K. Desorption branches are omitted here for calarity and are included in the Supporting Information. (b) Comparison of propylene/propane IAST selectivity for an equimolar binary mixture and propylene gravimetric uptake (298 K and 1 bar) for different porous materials. IAST selectivity of MOFs showing molecular sieving, which is not quantified here, is largely uncertain as a result of the negligible uptake of propane but is generally notably higher than 100. (b) is adapted from ref 18. Copyright [2020] American Chemical Society.

S13). The compound took up 3.16 mmol/g propylene at 298 K and 1 bar. In contrast, the uptake of propane was negligible (<0.3 mmol/g). Thus, HIAM-301 shows selective molecular exclusion of propane. Both the gravimetric and volumetric adsorption capacity of propylene on HIAM-301 (3.16 mmol/g, 93.0 v/v) are significantly higher than those for KAUST-7 (1.41 mmol/g, 56.8 v/v), Y-abtc (1.98 mmol/g, 64.6 v/v), and Co-gallate (1.79 mmol/g, 66.6 v/v) (Figure 2b). Ideal adsorption solution theory (IAST)[25,26] selectivity was calculated to be >150 between 0 and 1 bar at 298 K (Figure S14), which is substantially higher than that (20−60) of the top-performing MOFs featuring open metal sites and is comparable to those exhibiting molecular exclusion of propane, such as KAUST-7, Y-abtc, and Co-gallate.[18] The selective molecular exclusion behavior of HIAM-301 was confirmed by adsorption kinetics measurements as well as computational calculations. The adsorption of propylene reached equilibrium in 20 min while the uptake of propane was negligible ater 180 min under identical conditions (Figure S15). Computional modeling revealed that propane was excluded by HIAM-301 at the narrow window site with a diffusion energy barrier >100 kJ/mol. In contrast, the value for propylene is substantially lower (~40 kJ/mol), indicating it can easily pass through the window into the cage (Figure S16).

The high adsorpton selectivity and capacity of HIAM-301 is a notable advancement as the trade-off between adsorption capacity and selectivity represents the main challenge in this separation. Adsorbents showing selective molecular sieving would endow the highest possible selectivity. However, the stringent requirement on pore dimensions of the adsorbents largely restricts their pore volume, leading to a limited propylene uptake amount (pore volumes for KAUST-7, Y-abtc, and Co-gallate are 0.095, 0.18, and 0.21 cm^3/g, respectively). The larger pore volume of HIAM-301 (0.26 cm^3/g) contributes to a higher adsorption capacity for propylene. In addition, its optimal pore structure also allows for efficient packing of propylene in the cages with a packing density of propylene in HIAM-301 being 0.53 g/cm^3 (equivalent to ~87% of the liquid propylene density of 0.61 g/cm^3 at 225 K), thus noticeably higher than that for Co-gallate (0.36 g/cm^3). The isosteric heat of adsorption (Q_{st}) for propylene on HIAM-301 was calculated to be ~27 kJ/mol (Figure S17), slightly lower than that of JNU-3a[19] (~29.3 kJ/mol) and notably lower than those of the MOFs bearing open metal sites and KAUST-7, Y-abtc, and Co-gallate (in the range f 41−57 kJ/mol).[7,18,21] This is a significant advantage for practical applications where the energy required for regeneration can be reduced.

Column breakthrough experiments with an equimolar mixture of propane and propylene were conducted (Figure 3a). HIAM-301 exhibited clear separation. Propane eluted out at the beginning of the process, confirming the complete exclusion by the sorbent. In contrast, propylene was retained in the column for a substantially longer time of ~35 min/gram, with a dynamic propylene capacity of 46.4 cm^3/g. Three consecutive runs showed full retention of the separation

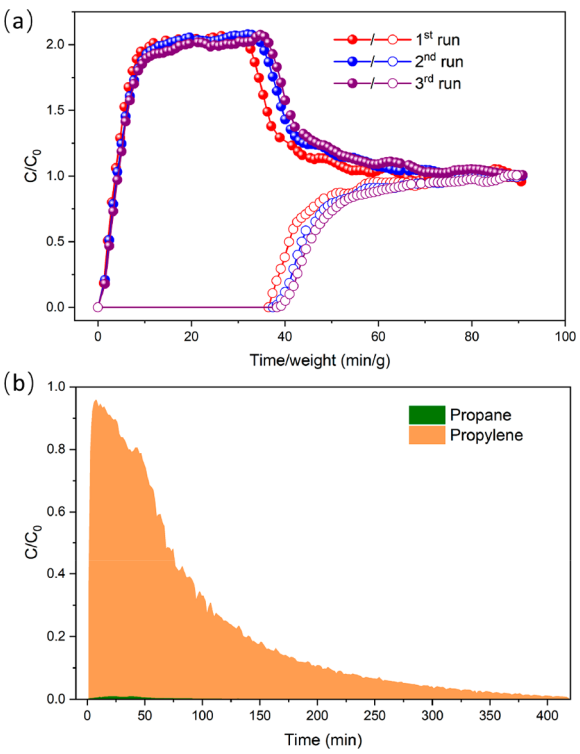

Figure 3. Separation of propane and propylene by HIAM-301. (a) Three consecutive runs of column breakthrough with a feed of an equimolar propane/propylene binary mixture at room temperature. Filled symbols, propane; open symbols, propylene. (b) Composition of desorbed gas following a column breakthrough experiment with a feed of binary mixture of propane/propylene = 5:95. Desorption was performed by heating the column from room temperature to 150 °C under nitrogen flow.

https://doi.org/10.1021/jacs.1c10423
J. Am. Chem. Soc. XXXX, XXX, XXX−XXX

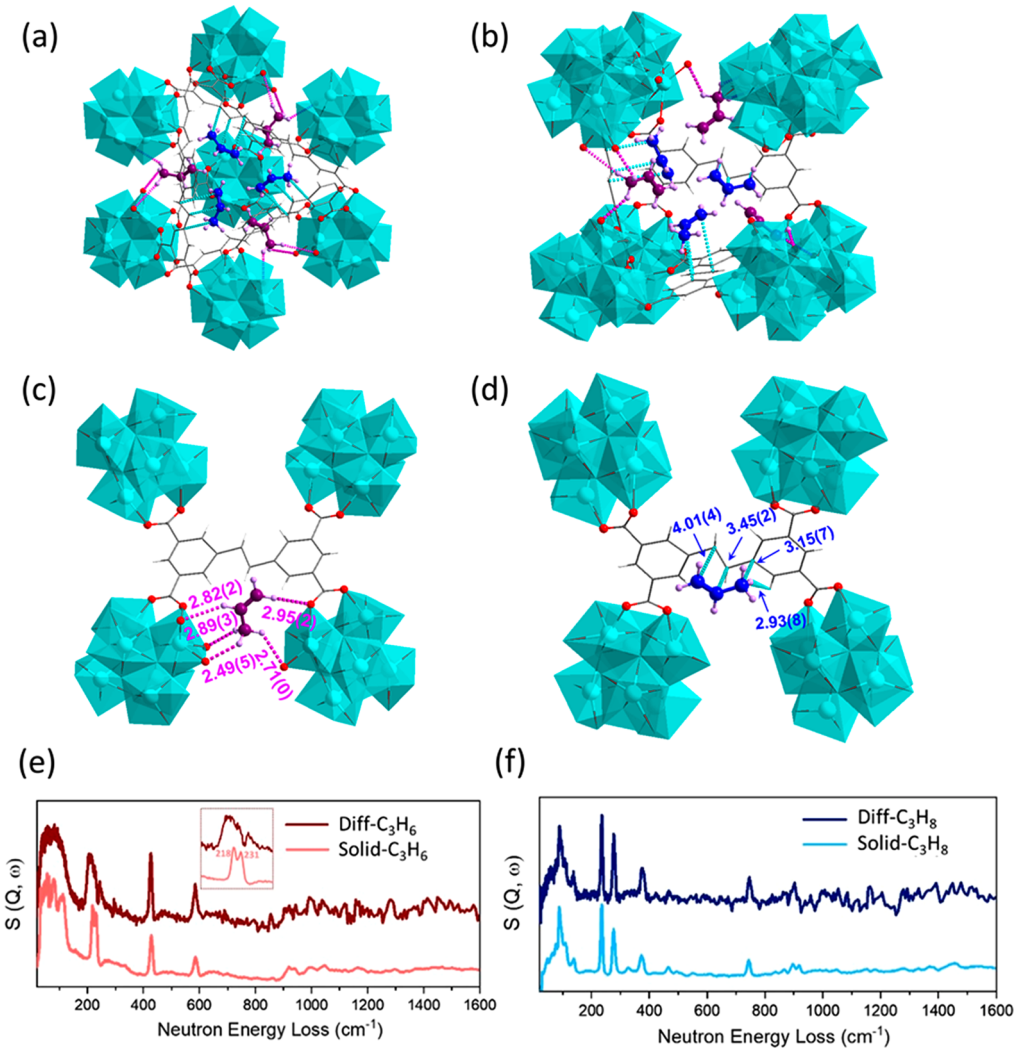

Figure 4. NPD and INS results for gas-loaded HIAM-301. (a and b) Views of two C_3D_6 sites in $Y_6(OH)_8(eedi)_3(DMA)_2{\cdot}2.26$ determined by NPD data at 10 K: (a) view along *c*-axis showing packing of the guest molecules in the pore and (b) view from the side of the pore showing the packing of the two C_3D_6 sites. (c) Details of the hydrogen bonding interactions between **Site I** C_3D_6 with the Y−O clusters. (d) π interactions between **Site II** C_3D_6 and the $eedi^{4-}$ ligand. Y, cyan; O, red; C_{ligand}, gray; H, white; C_{siteI}, purple; $C_{site\ II}$, blue; D, lilac; DMA cations are not shown for clarity. (e) Comparisons of the experimental difference INS spectrum of C_3H_6 and that of the solid C_3H_6 at 10 K. (f) Comparisons of the experimental difference INS spectrum of C_3H_8 and that of the solid C_3H_8 at 10 K.

capability of HIAM-301. A main challenge is to produce polymer-grade propylene (99.5+% purity) for industry. To this end, we carried out a column breakthrough measurement with a feed of propylene/propane = 95:5 (v/v), which can be easily obtained through simple distillation or other separation processes, and propylene with a purity of 99.6% and a recovery capacity of 38.5 cm^3/g was obtained at the outlet through a temperature swing adsorption process (Figure 3b). This confirms the feasibility of using HIAM-301 for the production of polymer-grade propylene.

Refinement of NPD data of activated HIAM-301, which was synthesized using deuterated DMF, confirmed the highly distorted pore structure and yielded three independent D-DMA sites in the cage near the window (in between two adjacent Y_6 vertexes) and thus would regulate the pore aperture of the MOF (Figure S18). NPD studies on C_3D_6-loaded HIAM-301 was subsequently performed with two different C_3D_6 loadings of $Y_6(OH)_8(eddi)_3(DMA)_2{\cdot}1.30C_3D_6$ and $Y_6(OH)_8(eddi)_3(DMA)_2{\cdot}2.33C_3D_6$ (Figures S19−S21). At both loadings, two C_3D_6 adsorption sites have been identified (Figure 4a−d). **Site I** is the predominant position with a higher occupancy, and the C_3D_6 molecule is anchored between two adjacent Y_6 clusters by strong hydrogen bonds ($D_{C_3D_6}\cdots O_{ligand}$ = 2.49−2.95 Å). **Site II** locates further toward the center of the pore and mainly interacts with the aromatic ligand through $\pi\cdots\pi$ stacking interactions ($C_{C_3D_6}\cdots C_{ligand}$ = 3.45−4.01 Å). The multiple host−guest interactions between C_3D_6 and the Y-MOF lead to the high uptake of propylene and enable the effective retention of propylene from gas mixtures under flow conditions.

To investigate the host−guest binding dynamics, INS measurements of the gas-loaded MOFs and pure gas molecules were conducted (Figure 4e,f and Figure S22). The INS spectra of C_3H_6 and C_3H_6 adsorbed in HIAM-301 (namely, Diff-C_3H_6, which was obtained by subtracting INS spectrum of bare HIAM-301 from that of the HIAM-301·0.8C_3H_6) are shown in Figure 4e. Sharp features are observed in both spectra below 700 cm^{-1}, indicating a reduced molecule recoil. An intense lattice mode for solid C_3H_6 was observed at a low energy

https://doi.org/10.1021/jacs.1c10423
J. Am. Chem. Soc. XXXX, XXX, XXX−XXX

(<140 cm^{-1}), which became an unresolved peak upon adsorption in HIAM-301, indicating the disappearance of the long-range order of the C_3H_6 molecules in the pore. In addition, the clearly resolved doublet at 218 and 231 cm^{-1} corresponding to in-phase and anti-phase torsion of C−CH_3 in solid C_3H_6 became a broadened peak covering a wider frequency range upon adsorption. This indicates that the interaction between adjacent C_3H_6 molecules in the solid state is broken when adsorbed in HIAM-301, and each −CH_3 group rotates according to its own local environment due to the strong interactions with the framework. In contrast, for C_3H_8, the difference INS spectrum shows almost identical features to that of the solid C_3H_8 (Figure 4f), indicating the absence of host−guest interactions, thus justifying its low uptake.

The efficient separation of propane and propylene remains a great challenge in the petrochemical industry. We have designed a **ftw**-type MOF, HIAM-301, featuring a distorted and optimal pore structure that allows for distinct adsorption of propylene and the total exclusion of propane. Having large sized inner cages, HIAM-301 offers the highest adsorption capacity for propylene compared to all previously reported adsorbents that exhibit a similar molecular exclusion of propane. Excellent adsorption selectivity and capacity of an adsorbent marks a significant advance for the challenging industrial spearation of propylene/propane. The capability of HIAM-301 for the dynamic separation and purification of propylene from propane has been confirmed by breakthrough measurements. Through NPD/INS analysis, we have also identified the domains of the DMA cations and adsorbed propylene molecules in HIAM-301 as well as the MOF−proplyene binding dynamics. This study not only demonstrates the power of pore structure optimization guided by reticular chemistry but also provides useful information and insight for the future development of target-specific sorbent materials capable of addressing most challenging problems in separation technology.

■ ASSOCIATED CONTENT

Supporting Information

The Supporting Information is available free of charge at https://pubs.acs.org/doi/10.1021/jacs.1c10423.

Discussions of experimental details and calculations, figures of construction of **ftw**-type MOF structures, geometry and orientation comparisons, PXRD patterns, TGA curves, adsorption−desorption isotherms, ^{1}H NMR spectrum, pore size distribution, IAST selectivity, adsorption rates, virial fittings, crystal structures, neutron powder diffraction patterns, Rietveld refinements, and INS spectra, and tables of details of crystal data, fitting parameters for Dual Site Langmuir−Freundlich isotherm model, and virial fitting parameters for propylene (PDF)

Accession Codes

CCDC 2087017−2087019 and 2087143 contain the supplementary crystallographic data for this paper. These data can be obtained free of charge via www.ccdc.cam.ac.uk/data_request/cif, or by emailing data_request@ccdc.cam.ac.uk, or by contacting The Cambridge Crystallographic Data Centre, 12 Union Road, Cambridge CB2 1EZ, UK; fax: +44 1223 336033.

■ AUTHOR INFORMATION

Corresponding Authors

Hao Wang − *Hoffmann Institute of Advanced Materials, Shenzhen Polytechnic, Shenzhen, Guangdong 518055, P. R. China;* orcid.org/0000-0001-7732-778X; Email: wanghao@szpt.edu.cn

Sihai Yang − *Department of Chemistry, University of Manchester, Manchester M13 9PL, United Kingdom;* orcid.org/0000-0002-1111-9272; Email: Sihai.Yang@manchester.ac.uk

Jing Li − *Hoffmann Institute of Advanced Materials, Shenzhen Polytechnic, Shenzhen, Guangdong 518055, P. R. China; Department of Chemistry and Chemical Biology, Rutgers University, Piscataway, New Jersey 08854, United States;* orcid.org/0000-0001-7792-4322; Email: jingli@rutgers.edu

Authors

Liang Yu − *Hoffmann Institute of Advanced Materials, Shenzhen Polytechnic, Shenzhen, Guangdong 518055, P. R. China; School of Chemistry and Chemical Engineering, South China University of Technology, Guangzhou 510640, P. R. China*

Xue Han − *Department of Chemistry, University of Manchester, Manchester M13 9PL, United Kingdom*

Saif Ullah − *Department of Physics and Center for Functional Materials, Wake Forest University, Winston-Salem, North Carolina 27109, United States;* orcid.org/0000-0001-8836-9862

Qibin Xia − *School of Chemistry and Chemical Engineering, South China University of Technology, Guangzhou 510640, P. R. China;* orcid.org/0000-0002-8563-6715

Weiyao Li − *Department of Chemistry, University of Manchester, Manchester M13 9PL, United Kingdom*

Jiangnan Li − *Department of Chemistry, University of Manchester, Manchester M13 9PL, United Kingdom*

Ivan da Silva − *ISIS Facility, STFC, Rutherford Appleton Laboratory, Chilton, Oxfordshire OX11 0QX, United Kingdom;* orcid.org/0000-0002-4472-9675

Pascal Manuel − *ISIS Facility, STFC, Rutherford Appleton Laboratory, Chilton, Oxfordshire OX11 0QX, United Kingdom*

Svemir Rudić − *ISIS Facility, STFC, Rutherford Appleton Laboratory, Chilton, Oxfordshire OX11 0QX, United Kingdom;* orcid.org/0000-0003-3023-8565

Yongqiang Cheng − *Neutron Scattering Division, Neutron Sciences Directorate, Oak Ridge National Laboratory, Oak Ridge, Tennessee 37831, United States;* orcid.org/0000-0002-3263-4812

Timo Thonhauser − *Department of Physics and Center for Functional Materials, Wake Forest University, Winston-Salem, North Carolina 27109, United States;* orcid.org/0000-0003-4771-7511

Complete contact information is available at: https://pubs.acs.org/10.1021/jacs.1c10423

Author Contributions

○L.Y. and X.H. contributed equally to this work.

Notes

The authors declare no competing financial interest.

https://doi.org/10.1021/jacs.1c10423
J. Am. Chem. Soc. XXXX, XXX, XXX−XXX

■ ACKNOWLEDGMENTS

The authors would like to thank the financial support from the National Natural Science Foundation of China (21901166), the Guangdong Natural Science Foundation (2019A1515010692), and Shenzhen Science and Technology Program (No. JCYJ20190809145615620, RCYX20200714114539243). The authors are grateful to the STFC/ISIS Facility for access to Beamlines TOSCA and WISH. Work by the U.S. teams was supported by the U.S. Department of Energy, Office of Science, Office of Basic Energy Sciences under Award DESC0019902.

■ REFERENCES

(1) Balogun, M. L.; Adamu, S.; Bakare, I. A.; Ba-Shammakh, M. S.; Hossain, M. M. CO_2 Assisted Oxidative Dehydrogenation of Propane to Propylene over Fluidizable MoO_3/La_2O_3-γAl_2O_3 Catalysts. *Journal of CO_2 Utilization* **2020**, *42*, 101329.

(2) Grande, C. A.; Rodrigues, A. E. Propane/Propylene Separation by Pressure Swing Adsorption Using Zeolite 4A. *Ind. Eng. Chem. Res.* **2005**, *44* (23), 8815−8829.

(3) Khalighi, M.; Chen, Y. F.; Farooq, S.; Karimi, I. A.; Jiang, J. W. Propylene/Propane Separation Using SiCHA. *Ind. Eng. Chem. Res.* **2013**, *52* (10), 3877−3892.

(4) Jarvelin, H.; Fair, J. R. Adsorptive separation of propylene-propane mixtures. *Ind. Eng. Chem. Res.* **1993**, *32* (10), 2201−2207.

(5) Zarca, R.; Ortiz, A.; Gorri, D.; Ortiz, I. Facilitated Transport of Propylene Through Composite Polymer-Ionic Liquid Membranes. Mass Transfer Analysis. *Chem. Prod. Process Model.* **2016**, *11* (1), 77.

(6) Xiong, Y.; Woodward, R. T.; Danaci, D.; Evans, A.; Tian, T.; Azzan, H.; Ardakani, M.; Petit, C. Understanding trade-offs in adsorption capacity, selectivity and kinetics for propylene/propane separation using composites of activated carbon and hypercrosslinked polymer. *Chem. Eng. J.* **2021**, *426*, 131628.

(7) Cadiau, A.; Adil, K.; Bhatt, P. M.; Belmabkhout, Y.; Eddaoudi, M. A metal-organic framework−based splitter for separating propylene from propane. *Science* **2016**, *353* (6295), 137.

(8) Adil, K.; Belmabkhout, Y.; Pillai, R. S.; Cadiau, A.; Bhatt, P. M.; Assen, A. H.; Maurin, G.; Eddaoudi, M. Gas/vapour separation using ultra-microporous metal−organic frameworks: insights into the structure/separation relationship. *Chem. Soc. Rev.* **2017**, *46* (11), 3402−3430.

(9) Furukawa, H.; Cordova, K. E.; O'Keeffe, M.; Yaghi, O. M. The Chemistry and Applications of Metal-Organic Frameworks. *Science* **2013**, *341* (6149), 1230444.

(10) Wang, H.; Liu, Y.; Li, J. Designer Metal−Organic Frameworks for Size-Exclusion-Based Hydrocarbon Separations: Progress and Challenges. *Adv. Mater.* **2020**, *32* (44), 2002603.

(11) Cui, W.-G.; Hu, T.-L.; Bu, X.-H. Metal−Organic Framework Materials for the Separation and Purification of Light Hydrocarbons. *Adv. Mater.* **2020**, *32* (3), 1806445.

(12) Schröder, M.; Li, J.; Han, X.; Kang, X.; Chen, Y.; Xu, S.; Smith, G. L.; Tillotson, E.; Cheng, Y.; McCormick McPherson, L.; Teat, S. J.; Rudic, S.; Ramirez-Cuesta, A. J.; Haigh, S. J.; Yang, S. Purification of propylene and ethylene by a robust metal-organic framework mediated by host-guest interactions. *Angew. Chem., Int. Ed.* **2021**, *60*, 15541−15547.

(13) Bloch, E. D.; Queen, W. L.; Krishna, R.; Zadrozny, J. M.; Brown, C. M.; Long, J. R. Hydrocarbon Separations in a Metal-Organic Framework with Open Iron(II) Coordination Sites. *Science* **2012**, *335* (6076), 1606.

(14) Geier, S. J.; Mason, J. A.; Bloch, E. D.; Queen, W. L.; Hudson, M. R.; Brown, C. M.; Long, J. R. Selective adsorption of ethylene over ethane and propylene over propane in the metal−organic frameworks M_2(dobdc) (M = Mg, Mn, Fe, Co, Ni, Zn). *Chemical Science* **2013**, *4* (5), 2054−2061.

(15) Li, K.; Olson, D. H.; Seidel, J.; Emge, T. J.; Gong, H.; Zeng, H.; Li, J. Zeolitic Imidazolate Frameworks for Kinetic Separation of Propane and Propene. *J. Am. Chem. Soc.* **2009**, *131* (30), 10368−10369.

(16) Lee, C. Y.; Bae, Y.-S.; Jeong, N. C.; Farha, O. K.; Sarjeant, A. A.; Stern, C. L.; Nickias, P.; Snurr, R. Q.; Hupp, J. T.; Nguyen, S. T. Kinetic Separation of Propene and Propane in Metal−Organic Frameworks: Controlling Diffusion Rates in Plate-Shaped Crystals via Tuning of Pore Apertures and Crystallite Aspect Ratios. *J. Am. Chem. Soc.* **2011**, *133* (14), 5228−5231.

(17) Peng, J.; Wang, H.; Olson, D. H.; Li, Z.; Li, J. Efficient kinetic separation of propene and propane using two microporous metal organic frameworks. *Chem. Commun.* **2017**, *53* (67), 9332−9335.

(18) Liang, B.; Zhang, X.; Xie, Y.; Lin, R.-B.; Krishna, R.; Cui, H.; Li, Z.; Shi, Y.; Wu, H.; Zhou, W.; Chen, B. An Ultramicroporous Metal−Organic Framework for High Sieving Separation of Propylene from Propane. *J. Am. Chem. Soc.* **2020**, *142* (41), 17795−17801.

(19) Zeng, H.; Xie, M.; Wang, T.; Wei, R.-J.; Xie, X.-J.; Zhao, Y.; Lu, W.; Li, D. Orthogonal-array dynamic molecular sieving of propylene/propane mixtures. *Nature* **2021**, *595* (7868), 542−548.

(20) Bai, Y.; Dou, Y.; Xie, L.-H.; Rutledge, W.; Li, J.-R.; Zhou, H.-C. Zr-based metal-organic frameworks: design, synthesis, structure, and applications. *Chem. Soc. Rev.* **2016**, *45*, 2327−2367.

(21) Wang, H.; Dong, X.; Colombo, V.; Wang, Q.; Liu, Y.; Liu, W.; Wang, X.-L.; Huang, X.-Y.; Proserpio, D. M.; Sironi, A.; Han, Y.; Li, J. Tailor-Made Microporous Metal−Organic Frameworks for the Full Separation of Propane from Propylene Through Selective Size Exclusion. *Adv. Mater.* **2018**, *30* (49), 1805088.

(22) Luebke, R.; Belmabkhout, Y.; Weseliński, Ł. J.; Cairns, A. J.; Alkordi, M.; Norton, G.; Wojtas, Ł.; Adil, K.; Eddaoudi, M. Versatile rare earth hexanuclear clusters for the design and synthesis of highly-connected ftw-MOFs. *Chemical Science* **2015**, *6* (7), 4095−4102.

(23) Xue, D.-X.; Cadiau, A.; Weseliński, Ł. J.; Jiang, H.; Bhatt, P. M.; Shkurenko, A.; Wojtas, L.; Zhijie, C.; Belmabkhout, Y.; Adil, K.; Eddaoudi, M. Topology meets MOF chemistry for pore-aperture fine tuning: ftw-MOF platform for energy-efficient separations via adsorption kinetics or molecular sieving. *Chem. Commun.* **2018**, *54* (49), 6404−6407.

(24) Yang, S.; Sun, J.; Ramirez-Cuesta, A. J.; Callear, S. K.; David, W. I. F.; Anderson, D. P.; Newby, R.; Blake, A. J.; Parker, J. E.; Tang, C. C.; Schröder, M. Selectivity and direct visualization of carbon dioxide and sulfur dioxide in a decorated porous host. *Nat. Chem.* **2012**, *4* (11), 887−894.

(25) Myers, A. L.; Prausnitz, J. M. Thermodynamics of mixed-gas adsorption. *AIChE J.* **1965**, *11* (1), 121−127.

(26) Zhang, Z.; Liu, J.; Li, Z.; Li, J. Experimental and theoretical investigations on the MMOF selectivity for CO_2 vs. N_2 in flue gas mixtures. *Dalton Transactions* **2012**, *41* (14), 4232−4238.

https://doi.org/10.1021/jacs.1c10423
J. Am. Chem. Soc. XXXX, XXX, XXX−XXX